

RESEARCH ARTICLE

Genomic features underlie the co-option of SVA transposons as cis-regulatory elements in human pluripotent stem cells

Samantha M. Barnada ^{1,2‡}, Andrew Isopi ^{3,4‡}, Daniela Tejada-Martinez¹, Clément Goubert ⁵, Sruti Patoori ¹, Luca Pagliaroli¹, Mason Tracewell ^{1,4}, Marco Trizzino ^{1*}

1 Department of Biochemistry and Molecular Biology, Sidney Kimmel Medical College, Thomas Jefferson University, Philadelphia, Pennsylvania, United States of America, **2** Genetics, Genomics and Cancer Biology PhD Program, Thomas Jefferson University, Philadelphia, Pennsylvania, United States of America, **3** Department of Microbiology and Immunology, Sidney Kimmel Medical College, Thomas Jefferson University, Philadelphia, Pennsylvania, United States of America, **4** Biochemistry and Molecular Pharmacology PhD Program, Thomas Jefferson University, Philadelphia, Pennsylvania, United States of America, **5** Department of Human Genetics, McGill University, Montreal, Quebec, Canada

‡ These authors share first authorship on this work.

* marco.trizzino83@gmail.com



OPEN ACCESS

Citation: Barnada SM, Isopi A, Tejada-Martinez D, Goubert C, Patoori S, Pagliaroli L, et al. (2022) Genomic features underlie the co-option of SVA transposons as cis-regulatory elements in human pluripotent stem cells. *PLoS Genet* 18(6): e1010225. <https://doi.org/10.1371/journal.pgen.1010225>

Editor: Cédric Feschotte, Cornell University, UNITED STATES

Received: March 25, 2022

Accepted: April 28, 2022

Published: June 15, 2022

Copyright: © 2022 Barnada et al. This is an open access article distributed under the terms of the [Creative Commons Attribution License](https://creativecommons.org/licenses/by/4.0/), which permits unrestricted use, distribution, and reproduction in any medium, provided the original author and source are credited.

Data Availability Statement: The original genome-wide data generated in this study have been deposited in the GEO database under accession code GSE192951.

Funding: M.T. is funded by NIH, grant nr.: R35GM138344. The funders played no role in the study design, data collection and analysis, decision to publish, or preparation of the manuscript.

Competing interests: The authors have declared that no competing interests exist.

Abstract

Domestication of transposable elements (TEs) into functional cis-regulatory elements is a widespread phenomenon. However, the mechanisms behind why some TEs are co-opted as functional enhancers while others are not are underappreciated. SINE-VNTR-Alus (SVAs) are the youngest group of transposons in the human genome, where ~3,700 copies are annotated, nearly half of which are human-specific. Many studies indicate that SVAs are among the most frequently co-opted TEs in human gene regulation, but the mechanisms underlying such processes have not yet been thoroughly investigated. Here, we leveraged CRISPR-interference (CRISPRi), computational and functional genomics to elucidate the genomic features that underlie SVA domestication into human stem-cell gene regulation. We found that ~750 SVAs are co-opted as functional cis-regulatory elements in human induced pluripotent stem cells. These SVAs are significantly closer to genes and harbor more transcription factor binding sites than non-co-opted SVAs. We show that a long DNA motif composed of flanking YY1/2 and OCT4 binding sites is enriched in the co-opted SVAs and that these two transcription factors bind consecutively on the TE sequence. We used CRISPRi to epigenetically repress active SVAs in stem cell-like NCCIT cells. Epigenetic perturbation of active SVAs strongly attenuated YY1/OCT4 binding and influenced neighboring gene expression. Ultimately, SVA repression resulted in ~3,000 differentially expressed genes, 131 of which were the nearest gene to an annotated SVA. In summary, we demonstrated that SVAs modulate human gene expression, and uncovered that location and sequence composition contribute to SVA domestication into gene regulatory networks.

Author summary

SINE-VNTR-Alus (SVAs) are the youngest group of transposons in the human genome, where ~3,700 copies are annotated. Nearly half of the SVAs annotated in the human genome are exclusive to our species. Many studies indicate that SVAs are among the most frequently co-opted TEs in human gene regulation, but the mechanisms underlying such processes have not yet been thoroughly investigated. Here, we filled this knowledge-gap by focusing on human induced pluripotent stem cells (iPSCs) and on a pluripotent-like cell line (NCCITs). Through the analysis of histone marks, gene expression profiles, and by means of genome editing (CRISPR-interference), we identified ~750 SVAs that work as enhancers and promoters in human pluripotent cells, and characterized a mechanism for SVA co-option involving the transcription factors OCT4 and YY1. With our CRISPR approach, we demonstrated that repressing the 750 active SVAs leads to alteration in the expression of ~3,000 genes.

Introduction

Transposable elements (TEs) are mobile DNA sequences that account for over 50% of the human genome, yet there is very limited knowledge on the extent of their impact on genome evolution, function, and disease.

Many elegant studies have proposed that TE sequences constantly reshape eukaryotic gene regulation [1–24] yet the underlying mechanisms are largely uncharacterized. Several TE types are active and replication competent in humans, and the genomic dispersal of these elements can affect the regulatory configurations of proximal host genes. For example, TE insertions may introduce novel cis-regulatory elements (CREs = enhancers, promoters, insulators) at the gene locus [8,13,14,16,17]. Alternatively, TE insertion can disrupt transcription factor binding sites (TFBS) within pre-existing CREs, thus attenuating or completely repressing nearby gene expression [25]. Additionally, insertion of TEs into coding sequences of genes may disrupt the open reading frames, and modify splicing sites [26–28]. Dysregulated gene expression due to TE insertions can lead to disease phenotypes as TE de-repression (i.e. de-methylation of TE sequences) is correlated with many neurological disorders and is a hallmark of multiple cancer types [29–40].

Over the last decade, the scientific community has begun to characterize the biological determinants of TE co-option in mammalian regulatory networks [8,13,14,17,20,41]. SINE-VNTR-Alus (SVAs) are the youngest human TEs. These transposons are composed of a 5' CCCTCT hexamer repeat, an Alu-like element, a variable number of tandem repeats (VNTR), a SINE element derived from an ancestral endogenous retrovirus (HERVK-10), and a poly-A tail [42]. Six main SVA subfamilies have been characterized (SVA-A through -F) and nearly half of the annotated ~3,700 copies are human-specific, including all the SVA-Es and -Fs.

Importantly, the SVAs are still actively transposing in the human genome by taking advantage of the L1-LINE machinery, and are among the most epigenetically de-repressed and transcriptionally upregulated TEs across a multitude of cancers and neurological disorders [17,24,26,33,43]. Given their young evolutionary age, SVAs provide a unique opportunity to elucidate how the human genome is evolving.

We, and others, have demonstrated that SVAs are frequently co-opted as functional enhancers and promoters in human and chimpanzee gene regulatory networks [16,17,20,24]. Yet, we have an incomplete understanding of the extent of this evolutionary process and the

underlying mechanisms. Why are some SVAs recruited as functional enhancers and others are not? What are the molecular properties underlying the regulatory potential of SVAs? Here, we answered these questions by exploring the highly permissive genomic environment of induced pluripotent stem cells (iPSCs) and NCCIT cells. The latter is a human cell line derived from an embryonal carcinoma which exhibits genomic properties comparable to human embryonic stem cells and iPSCs, including widespread de-methylation. These cells are particularly favorable for the study of transposable elements [18]. Compared to iPSCs, NCCITs are easier to manipulate and more suitable to perform Cas9-mediated genome editing experiments.

We demonstrate that ~750 SVAs are depleted of repressive histone marks (i.e. H3K9me3) in iPSCs and in NCCITs. We found that the transcriptionally active SVAs are significantly closer to genes and harbor more TFBS than those harboring the repressive H3K9me3 epigenetic modification. Moreover, when comparing the sequence of the de-repressed SVAs with the repressed SVAs, we detected an enrichment for a long DNA motif composed of flanking binding sites for YY1/2 and OCT4 within the de-repressed group. The former is a ubiquitously expressed transcriptional regulator, while the latter is an essential regulator of cell pluripotency. Further, the de-repressed SVAs are also enriched for individual (i.e. non-flanking) YY1 and OCT4 binding sites. We used Chromatin Immunoprecipitation followed by sequencing (ChIP-seq) to demonstrate that YY1 and OCT4 bind adjacently on many of the active SVAs. We leveraged CRISPR-interference (CRISPRi) to epigenetically repress active SVAs resulting in a loss of YY1 and OCT4 binding leading to massive alterations in gene expression.

Results

Human-specific SVAs are enriched in areas of de-repressed chromatin

We took advantage of publicly available H3K9me3 ChIP-seq data (paired-end long reads) generated in iPSCs [19] to assess to what extent SVAs are repressed in a pluripotent context. We only retained uniquely mapping high quality reads (Samtools q10 filtering). This analysis revealed that of all the SVAs annotated in the human genome (N = 3,734; hg19 assembly), approximately 80% (2,983) are decorated with this repressive histone methylation in iPSCs (Fig 1A). Conversely, 751 SVAs were depleted of H3K9me3, indicating that they are de-repressed (Fig 1A).

Next, we wanted to compare the iPSC findings with data generated in NCCITs in our laboratory. As mentioned, NCCITs have pluripotent characteristics but compared to human iPSCs and embryonic stem cells, the NCCITs are significantly easier to manipulate and have high transfection efficiency, which makes them suitable for CRISPR experiments. Thus, we performed ChIP-seq for H3K9me3 to profile repressed SVA regions in NCCITs. To ensure high-quality read mappability of repetitive regions we sequenced 100 bp long paired-end reads and upon mapping, only retained the uniquely mapping high quality reads (Samtools q10 filtering). Notably, the SVA methylation pattern previously observed in iPSCs was perfectly recapitulated in NCCITs (Fig 1B and 1C). These findings indicate that NCCITs share a similar TE epigenetic landscape with iPSCs making them a suitable model to study stem cell genomics, and support that 751 SVAs are de-repressed in pluripotent environments (hereafter “de-repressed SVAs”; S1 Data).

We wanted to ensure that the lack of H3K9me3 signal on the de-repressed SVAs was not a consequence of mapping limitations, in that the youngest SVAs may be too similar to one another to allow for unique read mapping. To test this hypothesis, we looked at another histone modification. Specifically, we took advantage of publicly available H3K27ac ChIP-seq data (100bp paired-end) generated in NCCITs by the Wysocka laboratory [18]. H3K27ac usually decorates active cis-regulatory elements and we surmised that de-repressed SVAs may be

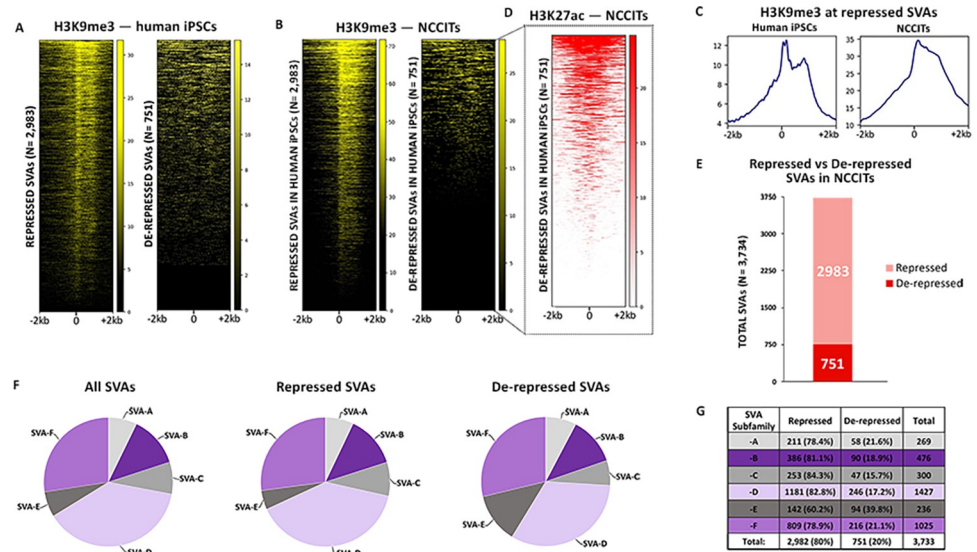


Fig 1. 751 human SVAs are active in human pluripotent cells. (A) Heatmaps depicting H3K9me3 ChIP-seq signal at all human SVAs in iPSCs. (B) ChIP-seq for H3K9me3 in human NCCITs at SVA regions previously classified as repressed and de-repressed in human iPSCs. (C) Average profiles of H3K9me3 enrichment at SVAs repressed in human iPSCs and NCCITs. (D) ChIP-seq for H3K27ac in NCCIT cells. The heatmap is centered on the 751 de-repressed SVAs. (E) Barplot representing the number of total repressed and de-repressed human SVAs (i.e. SVAs decorated with H3K9me3 versus lacking H3K9me3). 2982 of the ~3700 human SVAs were repressed, while 751 were de-repressed. (F) & (G) Human-specific SVAs, subfamilies SVA-E and -F are enriched within the de-repressed SVA population.

<https://doi.org/10.1371/journal.pgen.1010225.g001>

transcriptionally active and therefore should exhibit ChIP-seq signal for this histone mark. This analysis revealed that the large majority of the de-repressed SVAs (636/751) are decorated with H3K27ac, which suggests they are in an active regulatory state, and that they are “mappable” with uniquely mapped reads (hereafter “active SVAs”; Fig 1D). Additionally, 120 SVAs were not marked with H3K9me3 or H3K27ac. We attribute this pattern to potential mappability issues, and did not consider this SVA subset for downstream analyses. Overall, these data suggest that approximately 20% of all SVAs are located within transcriptionally de-repressed and active chromatin in iPSCs and in stem cell-like NCCITs (Fig 1A–1E).

SVAs can be further categorized into six evolutionarily conserved subfamilies (SVA-A through -F), two of which (SVA-E, -F, plus the F1 subgroup) are human-specific. We investigated the subfamily composition of the de-repressed and repressed SVAs and observed that human-specific SVA subfamilies -E and -F (including F1) were significantly enriched in the de-repressed group (Fisher’s Exact Test $p < 1.0 \times 10^{-5}$; Fig 1F). In particular, ~40% of the SVA-Es were found in a de-repressed state, as compared to an average of ~19% for all the other families (Fisher’s Exact Test $p < 2.2 \times 10^{-16}$; Fig 1G). In summary, these findings indicate that young, human-specific SVAs are enriched not only in de-repressed chromatin, but also in active regions in NCCIT cells.

Sequence location and composition underlie SVA activation

We aimed to investigate the specific genomic features underlying the selective de-repression of SVAs. First, we reasoned that active SVAs preferentially located near coding genes could be co-opted as active cis-regulatory elements. We used the Genecode_v33 annotations and calculated the distance from the nearest transcription start site (TSS) for both repressed and active SVAs. We observed that active SVAs are significantly closer to coding genes when compared

to the repressed SVAs (Wilcoxon's Rank Sum Test $p < 2.2 \times 10^{-16}$; Fig 2A). Namely, the active SVAs are located approximately 10 kb closer to the nearest TSS than the repressed SVAs (Fig 2A).

Next, we surmised that SVA de-repression may be a consequence of gene regulatory activity. Consistent with this hypothesis, we found that relative to the repressed SVAs, active SVAs were significantly closer to TFBS as defined by the Encode Consortium (Wilcoxon's rank-sum test $p = 2.84 \times 10^{-7}$; Fig 2B). Further, the active SVAs directly overlap a TFBS three times more frequently than the repressed SVAs (Fig 2B). These data suggest that the active SVAs have a higher likelihood of exhibiting gene-regulatory activity.

To further explore this hypothesis, we performed sequence-based computational motif analysis on the de-repressed SVAs using HOMER, with the repressed SVAs as the background control. With this approach, we identified an enrichment for a long motif composed of flanking YY1/2 and OCT4 binding sites in the de-repressed SVAs (Fig 2C). YY1/2 are ubiquitously expressed transcriptional regulators, while OCT4 is one of the transcription factors essential for pluripotency maintenance. The YY1-OCT motif is found seven times more frequently in the de-repressed SVAs than in the repressed ones. Importantly, not only is the flanking YY1-OCT4 motif enriched, but also individual (i.e. non-flanking) YY1 and OCT4 motifs are enriched in the de-repressed SVAs as compared to the repressed ones. For instance, the OCT4 motif alone is found in 12% of the de-repressed SVAs, as opposed to 1% of repressed SVAs.

Additionally, we identified an enriched CEBPA motif (Fig 2C). We conducted the opposite analysis, by looking for motifs enriched in repressed SVAs (using de-repressed as a background) and found several enriched motifs, including: SMAD3, KLF5 and several Krüppel-associated box (KRAB) domain-containing zinc-finger proteins (KZFPs).

Repression of conventionally de-repressed SVAs has global consequences on gene expression

Since our results indicate that ~20% of all SVAs may act as functional CREs in NCCITs, we aimed to validate our ChIP-seq data and computational predictions with a functional approach. We utilized CRISPRi to repress the 751 de-repressed SVAs. We leveraged the piggy-Bac transposon system (Systems Bioscience) to generate NCCIT cells with tetracycline-inducible expression of a functionally dead Cas9 (dCas9) fused to a repressive KRAB domain. We subsequently knocked-in two previously validated [20] single guide RNAs (sgRNAs) that simultaneously target approximately 80% of all the SVAs annotated in the human genome (Fig 3A). The sgRNAs target the dCas9-KRAB to de-repressed SVAs leading to the deposition of the repressive histone methylation, H3K9me3, by the KRAB domain (Fig 3A). This NCCIT cell line exhibiting tetracycline-inducible dCas9-KRAB expression and constitutive dual sgRNA expression is hereafter referred to as SCi-NCCITs (i.e. SVA-CRISPRi-NCCITs). We treated the SCi-NCCITs with doxycycline for 72 hours to robustly induce dCas9-KRAB activation and function (Fig 3B). Activation of dCas9-KRAB led to the accumulation of repressive H3K9me3 modifications on 620 of the 751 SVAs originally de-repressed in NCCITs (Fig 3C and 3D). Importantly, this further demonstrates that reads can be uniquely mapped on this group of SVAs.

To assess the impact of global SVA repression on genome-wide gene expression, we performed RNA-sequencing on the SCi-NCCITs in the presence and absence of doxycycline treatment (three replicates per condition). We identified 3,085 genes as differentially expressed upon induction of SVA repression ($FDR < 0.05$; S2 Data), of which 1,596 were identified as upregulated and 1,489 as downregulated (Fig 4A). The sgRNAs used for this experiment were originally designed to target a DNA sequence shared by SVAs with the LTR5Hs family [20].

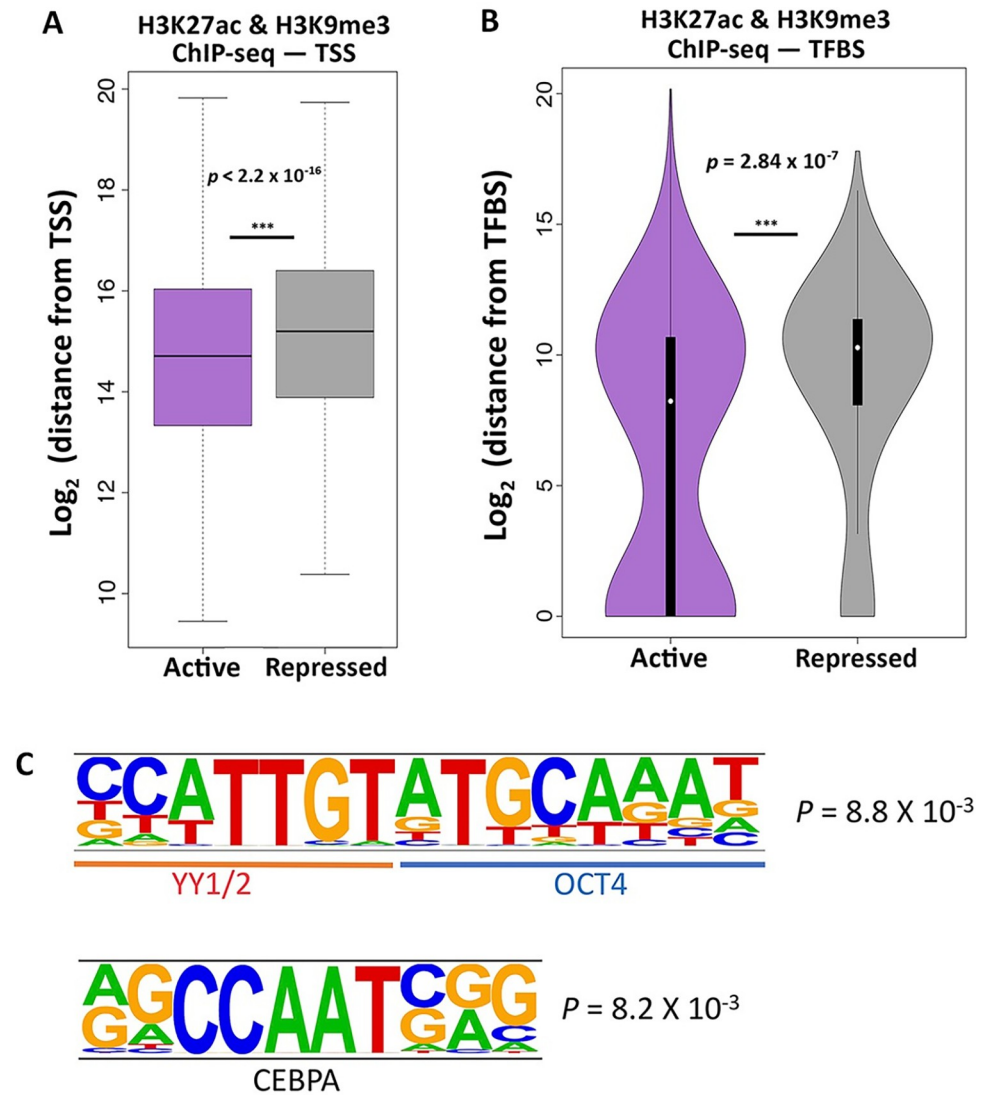


Fig 2. Specific genomic features characterize the de-repressed SVAs. (A) SVAs in an active configuration are approximately 10 kb closer to TSS than SVAs in a repressed configuration (Wilcoxon’s Rank Sum Test $p < 2.2 \times 10^{-16}$). (B) Active SVAs are significantly closer to, and directly overlap with, TFBS three times more than repressed SVAs (Wilcoxon’s rank-sum test $p = 2.84 \times 10^{-7}$). (C) Motif analysis performed on the de-repressed SVAs shows enrichment for consecutive YY1/2 and OCT4 motifs. A CEBPA motif was also enriched.

<https://doi.org/10.1371/journal.pgen.1010225.g002>

Given this premise, we restricted our analysis exclusively to genes putatively associated with human SVAs (i.e. considering only the genes that represent the closest gene to an annotated SVA). Overall, 131 of the 3,085 differentially expressed genes represented the closest gene to an SVA (Fig 4B), 101 of which were specifically near a de-repressed SVA. This number is significantly higher than expected by chance (Fisher’s Exact Test $p < 0.001$), suggesting that the expression of most of these 131 genes is likely under the direct control of SVAs. Importantly, 109 of the 131 SVA-regulated genes (83.2%) were downregulated upon doxycycline treatment (Fig 4B), indicating that SVA de-repression is necessary for gene activation.

We then assessed if any of the differential gene expression is due to repressing LTR5Hs since the sgRNAs also target DNA sequences in this TE family. Only 120/3,085 differentially expressed genes represented the closest gene to an LTR5H. Additionally, we detected very

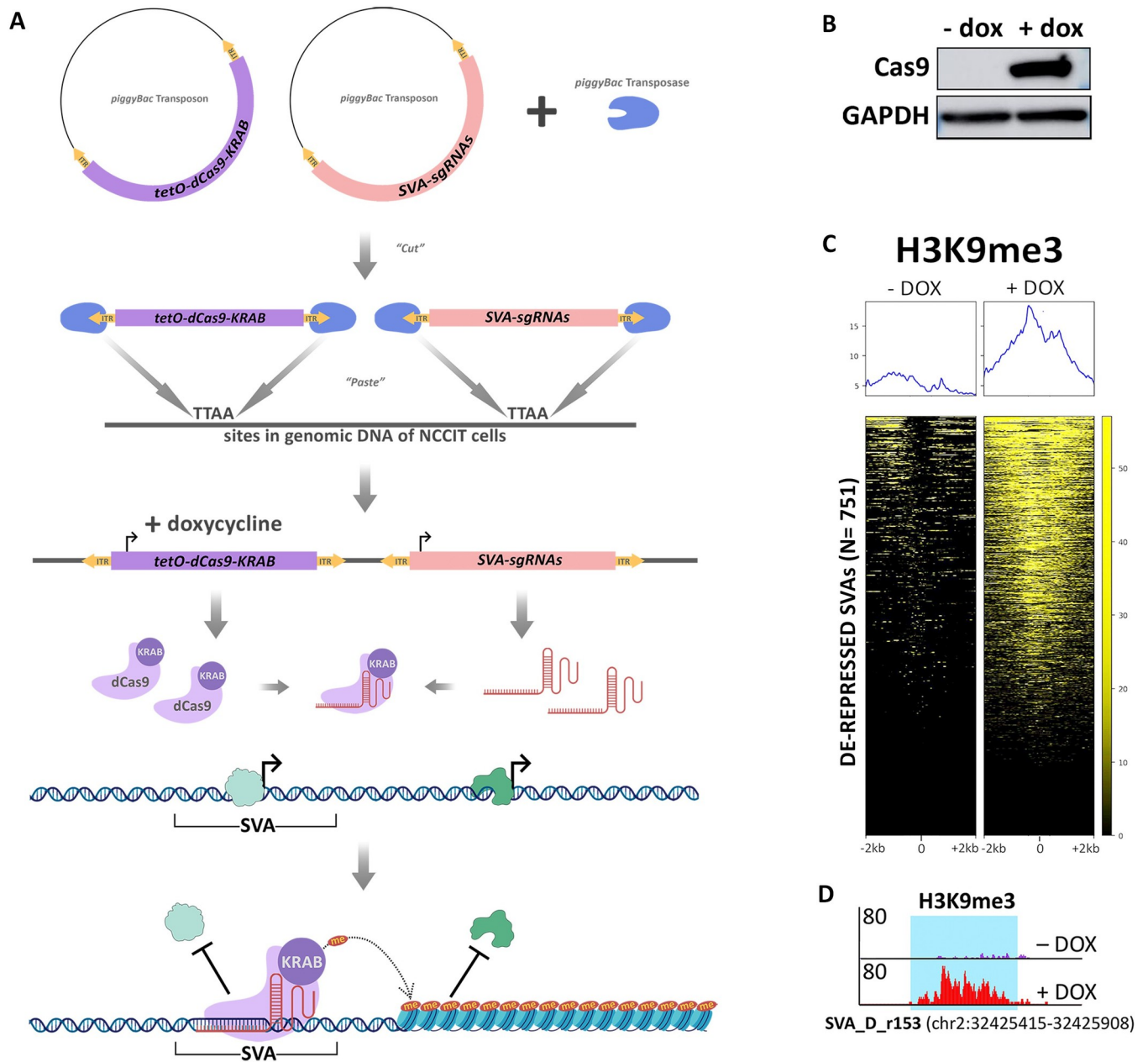


Fig 3. Epigenetic manipulation of NCCITs via CRISPRi results in SVA repression. (A) Schematic of the generation of the Sci-NCCIT line (created with BioRender.com). (B) Cas9 immunoblot displaying activation of dCas9-KRAB 72 hours post-doxycycline induction. (C) H3K9me3 ChIP-seq heatmap of the Sci-NCCITs shows increased H3K9me3 signal post-doxycycline treatment. (D) Genome browser screenshot displaying increased H3K9me3 before and after treatment with doxycycline at a de-repressed SVA-D.

<https://doi.org/10.1371/journal.pgen.1010225.g003>

minimal overlap (8 genes in total) between the differentially expressed genes near LTR5Hs and the differentially expressed genes near SVAs. These analyses ensure that the alterations in gene expression are due to the repression of SVAs and not LTR5Hs. In summary, these data indicate that the SVAs directly regulate the expression of at least 130 genes and that SVA repression may contribute to the differential expression of up to ~2,800 genes, potentially as a cascade effect.

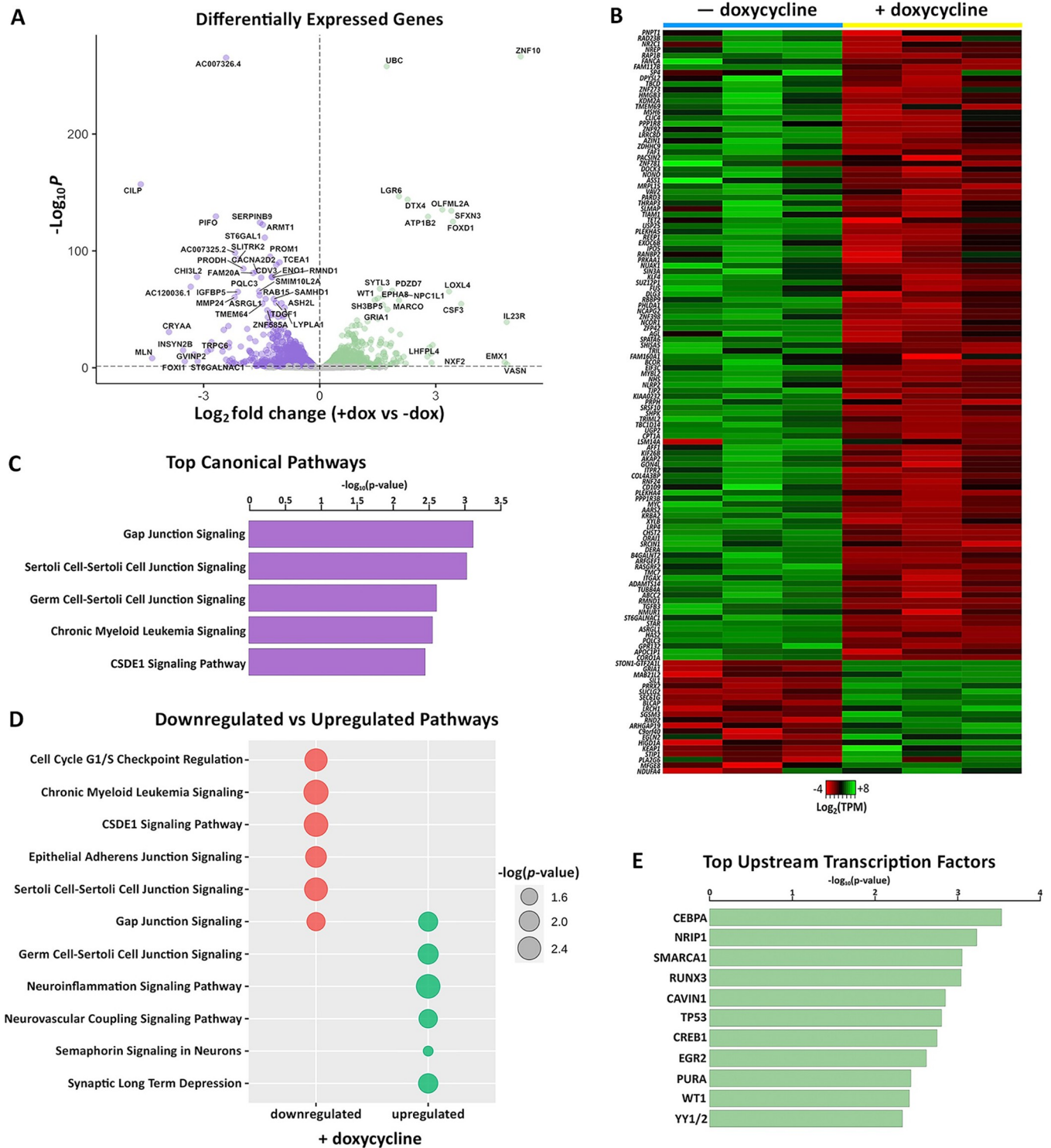


Fig 4. CRISPRi-mediated repression of conventionally de-repressed SVAs results in aberrant gene expression. (A) Volcano plot showing genes differentially expressed in SCi-NCCITs after doxycycline treatment (purple = downregulated genes; green = upregulated genes). (B) Heatmap of 131 genes that are differentially expressed post-doxycycline treatment and also represent the nearest gene to an SVA. (C) Top canonical pathways predicted by IPA for the 131 genes differentially expressed after doxycycline treatment. (D) Canonical pathways predicted by IPA for the 111 downregulated (red) and 20 upregulated (green) genes. (E) Top upstream regulators/transcription factors predicted by IPA for the 131 genes differentially expressed after doxycycline treatment.

<https://doi.org/10.1371/journal.pgen.1010225.g004>

We performed Ingenuity Pathway Analysis (IPA) on the 131 SVA-regulated genes and found an enrichment for gap junction signaling processes including Gap Junction Signaling, Sertoli Cell-Sertoli Cell Junction Signaling, and Germ Cell-Sertoli Cell Junction Signaling (Fig 4C and 4D). These processes are important during gametogenesis and given that NCCIT cells retain pluripotency-like characteristics, we speculate that co-opted SVAs could play a role in regulating germ line development and gametogenesis. However, it is important to note that the NCCIT cell line is derived from an embryonal testicular carcinoma, and this could bias our IPA. Nonetheless, recent studies have corroborated an SVA contribution in germ cells and showed that in human primordial germ cells, SVA sites are largely hypomethylated and genes proximal to SVAs are expressed at a higher level compared to embryonic stem cells [20,44,45]. Additionally, SVA transcription and retrotransposition are specifically seen in both human spermatozoa [46] and oocytes [47].

We next used IPA to look for top upstream transcriptional regulators of the 131 SVA-associated genes. This analysis identified transcription factors previously highlighted by the motif analyses (CEBPA and YY1/2), along with several others including SMARCA1, CREB1, and WT1 (Fig 4E). While YY1 is an essential ubiquitous developmental regulator [48], CEBPA is a regulator of differentiation in the hematopoietic [49] and adipocyte [50] lineages, and is involved in gametogenesis. SMARCA1 is a chromatin remodeler [51], CREB1 plays a role in both steroidal [52] and non-steroidal [53] female hormonal stimulation, and WT1 is involved in urogenital specification distinctively associated with the differentiation of Sertoli cells [54]. These data suggest a possible SVA contribution to germ line developmental processes and demonstrates the genome-wide impact of SVA repression on gene expression.

YY1 and OCT4 mediate SVA regulatory activity

Since our motif analysis revealed that de-repressed SVAs are enriched for adjacent YY1/2-OCT4 binding motifs and given that many differentially expressed genes were YY1/2 targets, we performed ChIP-seq for YY1 and OCT4 in SCi-NCCITs with and without doxycycline treatment. As done previously for the histone modification ChIP-seq, we sequenced 100 bp long paired-end reads to ensure high mappability efficiency.

These experiments revealed that under normal conditions (i.e. no doxycycline treatment) YY1 and OCT4 bind 288 and 54 SVAs, respectively (Fig 5A and 5B). Specifically, we identified two different clusters of YY1 binding: one located in the *Alu*-like region (Fig 5A top cluster), and a second near the start of the SINE element, likely in proximity of the HERVK10-derived promoter in the SINE region (Fig 5A second cluster). OCT4 binding was limited to this second region, whereas we did not detect binding for this transcription factor in the *Alu*-like region (Fig 5B). The SVAs bound by YY1 and OCT4 were all de-repressed SVAs decorated with H3K27ac. Importantly, binding of both YY1 and OCT4 was significantly attenuated upon SVA repression via CRISPRi (Fig 5A and 5B). We observed a significant overlap with 33 SVAs bound by both YY1 and OCT4 in the SINE region. In this case, the binding of the two transcription factors was sequential (i.e. one next to each other) as originally predicted by our motif analysis (Fig 5C). This pattern was found in de-repressed SVAs of all the main families (SVA-A through -F).

Finally, we leveraged the nearest TSS approach to determine the closest gene to each of the SVAs bound by YY1 and/or OCT4. Using our RNA-seq data, we investigated whether loss of YY1 and OCT4 binding altered the expression of neighboring genes. Notably, 44 of 288 genes located near YY1-bound SVAs and 24 of 54 genes located near OCT4-bound SVAs were differentially expressed upon CRISPRi-induced SVA repression (Fig 5D). Interestingly, of the 6 genes upregulated upon doxycycline treatment, 4 were located near SVAs bound exclusively

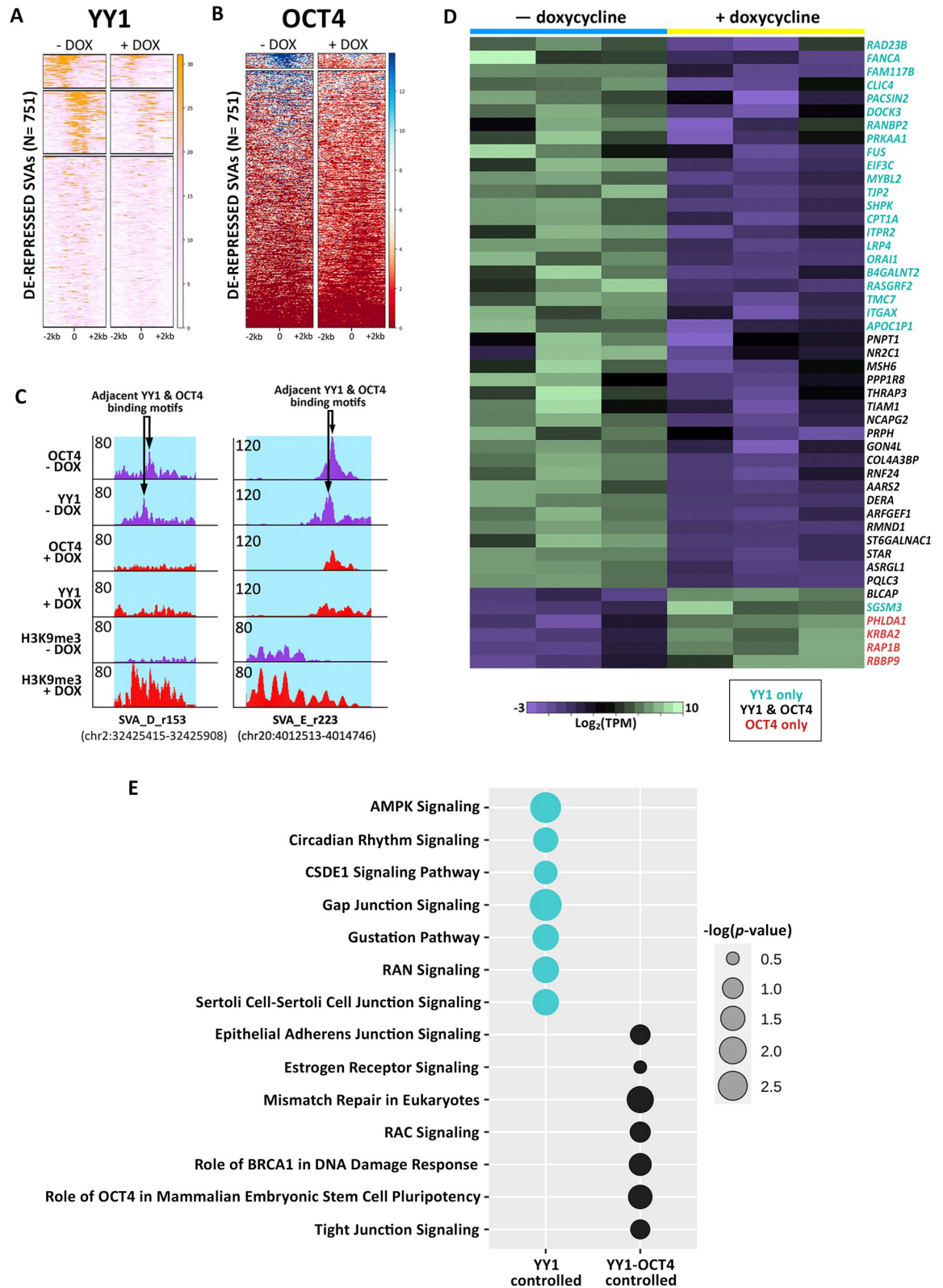


Fig 5. Individual and sequential binding of YY1 and OCT4 contributes to SVA regulatory activity. (A) YY1 ChIP-seq signal at the 751 de-repressed SVAs before and after doxycycline treatment. (B) OCT4 ChIP-seq signal at the 751 de-repressed SVAs before and after doxycycline treatment. (C) Genome browser screenshot displaying the sequential binding of YY1 and OCT4 at a truncated, de-

repressed SVA-D and a full-length, de-repressed, human-specific SVA-E. Upon doxycycline induction, the binding of both transcription factors is lost, while H3K9me3 signal is gained. The full length SVA-E is located near the gene *RNF24* (specifically 18kb from the TSS), which is downregulated upon CRISPRi mediated SVA repression ($\log_{2}FC = -0.56$; Adjusted $p = 9.14 \times 10^{-11}$) (D) Heatmap of 47 genes that are differentially expressed upon doxycycline treatment and regulated by YY1 and/or OCT4 (Black: YY1 and OCT4, Teal: YY1 only, Red: OCT4 only). (E) Canonical pathways predicted by IPA for the SVA-regulated genes that are differentially expressed upon doxycycline treatment and regulated by YY1-only (teal) and YY1-OCT4 (black).

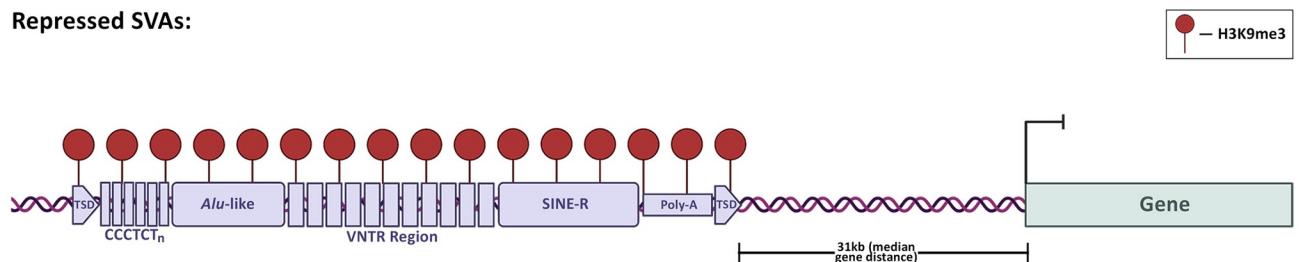
<https://doi.org/10.1371/journal.pgen.1010225.g005>

by OCT4 (Fig 5D). Overall, 85% of the genes (28/33) located near SVAs that were bound by both YY1 and OCT4 were differentially expressed upon CRISPRi-induced SVA repression (Fig 5D). This suggests that synergistic binding of these two transcription factors on the SVA sequence is important for the regulatory activity driven by these transposable elements (Figs 5D and 6). Pathway Analysis revealed that the genes regulated by the cooperative YY1-OCT4 binding (and by OCT4-only) are enriched for processes related to pluripotency and DNA repair (Fig 5E). Conversely, the genes bound by YY1-only are enriched for processes related to germline development (Fig 5E).

Discussion

SVAs are evolutionarily young transposable elements, which colonized the great ape genomes in the last 10–15 million years. In fact, they are not found in gibbons whose lineage split from the remaining apes ~17 million years ago [55]. Interestingly, the gibbon genome has been independently colonized by a distinct family of transposons called LAVAs (LINE-AluSz-

Repressed SVAs:



Active SVAs:

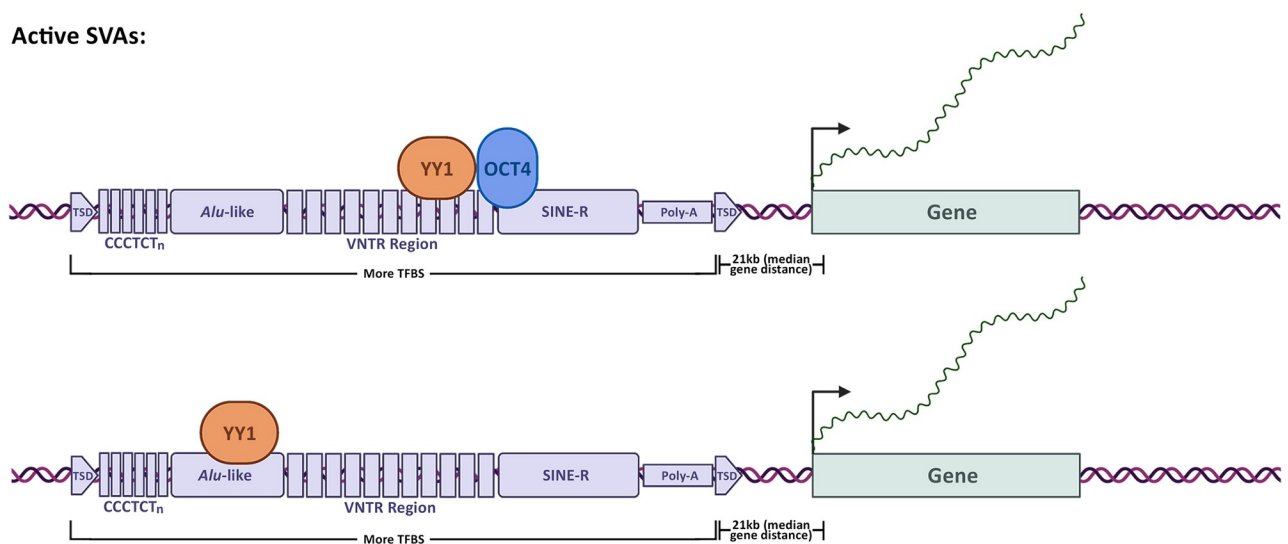


Fig 6. Model for SVA co-option in human pluripotent stem cell gene regulation. This figure was created with BioRender.com.

<https://doi.org/10.1371/journal.pgen.1010225.g006>

VNTR-Alu) [56,57]. Notably, SVA and LAVA structures are similar, and both have shown high cis-regulatory potential and massive co-option into gene regulatory networks [16,17,20,57]. However, the mechanisms underlying SVA and LAVA domestication and recruitment into primate gene regulatory networks have not been explored in depth.

Here, we aimed at elucidating such mechanisms, focusing specifically on SVAs and stem cells. We show that ~20% of all the human SVAs are found in a de-repressed chromatin state in iPSCs and in NCCITs, with a near perfect overlap between the two cell types. Most of these de-repressed SVAs were also decorated with histone modifications characteristic of active enhancers and promoters (H3K27ac), suggesting that their de-repression is associated with cis-regulatory activity. This pattern may indicate that either the SVAs are enriched in regions that were already transcriptionally active before their insertion, or that the SVAs themselves dictated the epigenetic landscape as a consequence of their sequence. A body of literature has emerged supporting the contribution of specific TE families to the dispersion of TFBS and cis-regulatory elements in the eukaryotic genomes [58]. This can happen in multiple ways: TEs already harbor the TFBS before the transposition event, or they gain TFBS afterwards as a consequence of new mutations. In the former case, if TEs harboring TFBSs insert near genes, this will increase the likelihood for the TE to be co-opted as an enhancer/promoter and thus lose repressive H3K9me3 and gain H3K27ac. Consistent with this scenario, it is estimated that in human embryonic stem cells, ~20% of the TFBSs for pluripotency factors are located within transposable elements [8,58,59,60].

The youngest SVAs (which are human-exclusive), and especially the SVA-Es, are the most enriched among the active copies. To this end, we speculate that the older SVAs accumulated genetic mutations over time, hampering their regulatory potential. Alternatively, the human genome may be adapted to silence older transposons, and this may have affected copies with higher regulatory potential.

According to our data, SVA location and sequence composition are the best predictors of cis-regulatory activity. Active SVAs are, on average, 10 kb closer to genes than the repressed ones. This is likely due to the fact that the chromatin environment near gene loci may be more frequently in an accessible and de-repressed state and is thus more suitable for co-option of novel cis-regulatory elements. Moreover, a shorter distance from the nearest TSS may facilitate the tri-dimensional interaction between the SVA-derived enhancer and the gene promoter. This is also in line with a recent study that demonstrated that eQTL-rich TEs tend to be significantly closer to genes than eQTL-poor TEs [25].

We show that active SVAs host a significantly higher number of TFBS than the repressed ones. This coincides with many studies suggesting that TE exaptation into gene regulatory networks is largely driven by the evidence that they propagate TFBS across the genome [60]. We demonstrate that a long motif with flanking YY1/2-OCT4 binding sites is enriched in de-repressed SVA copies relative to repressed SVAs. This may mediate their function in gene regulatory networks of stem and stem-like cells. In fact, OCT4 is one of the four Yamanaka factors [61] essential for pluripotency maintenance. YY1 is one of the major transcriptional regulators in human cells; it is ubiquitously expressed across all cell-types and performs many different functions in transcriptional regulation, including transcriptional activation, repression, as well as mediation of enhancer-promoter looping [62]. To this regard, over 40% of the SVAs de-repressed in iPSCs and NCCITs are bound by YY1, OCT4, or both. Importantly, when both are present, they bind alongside each other as predicted by computational motif analysis. As expected, depositing repressive histone methylation (H3K9me3) on the SVA locus nearly abolishes the binding of these two transcription factors near SVAs, leading to an alteration of nearby gene expression. In fact, even when restricting the analysis to the genes that are located near SVAs, repressing 620 of the 751 SVAs normally active in NCCITs results in 131

differentially expressed genes. The expression of most (88%) of these genes is attenuated with the repression of the nearby SVA, further supporting the enhancer activity provided by these transposons. These genes include important regulators of cell pluripotency and cell differentiation, such as *MYC*, *MYBL2*, *FUS*, *ITGAX*, *SP4* and several others. We remark that this analysis was very conservative. In fact, given the nature of the sgRNAs that we chose, which target both SVAs and LTR5Hs, we exclusively focused on the nearest gene to an SVA transposon, and thus the number of genes affected by distal SVA repression is likely much higher.

Finally, repressing SVAs did not result in any obvious alteration in cellular phenotypes, although we cannot rule out that a longer experiment (i.e. with cells collected more than 72 hours post doxycycline treatment) may result in alterations in cell viability/proliferation as a consequence of SVA-repression. Future studies may assess longer term SVA repression, focusing on the ability of iPSCs to act as pluripotent cells upon sustained repression of the SVA-derived enhancers. In summary, in this study we provide further evidence that SVA transposons are an important component of the human gene regulatory networks, specifically in stem and stem-like cells. We propose a potential mechanism underlying this cis-regulatory activity where SVA location and sequence composition regulate this co-option. Additional studies are required to determine if the YY1-OCT4 combination is a driver of SVA regulatory activity only in pluripotent cells or, alternatively, in a broader, more universal context. In this study most genomics experiments were conducted in NCCIT cells. Further genomic studies in human iPSCs will be necessary to confirm the proposed mechanism.

Materials and methods

Antibodies and sgRNAs

YY1 ChIP-seq: Cell Signaling Technology D5D9Z/46395S (15ug per ChIP). OCT4 ChIP-seq: Abcam ab181557 (15ug per ChIP). H3K27me3 ChIP-seq: Abcam ab8898 (3ug per ChIP). Cas9 Western Blot: Active Motif 61757 (1:100). GAPDH Western Blot: Cell Signaling Technology D16H11/5174 (1:1000). Anti-Rabbit IgG, HRP-linked Western Blot: Cell Signaling Technology 7074 (1:10000). Anti-Mouse IgG, HRP-linked Western Blot: Cell Signaling Technology 7076 (1:10000). The two sgRNAs were designed and used in a previous study [20]: sgRNA1: 5' CTCCCTAATCTCAAGTACCC 3'; sgRNA2: 5' TGTTTCAGAGAGCACGGGGT 3'.

NCCIT cell line culture

The NCCIT cell line (ATCC) was maintained in RPMI media supplemented with 10% tet-free FBS, 1% penicillin-streptomycin solution, and 1% L-glutamine and incubated at 5% CO₂, 20% O₂ at 37°C.

ChIP-sequencing

All samples from different conditions were processed together to prevent batch effects. Between 10–15 million cells were cross-linked with 1% formaldehyde for 5 minutes at room temperature, quenched with 125 mM glycine, harvested, and washed twice with 1x PBS. The fixed cell pellet was resuspended in ChIP lysis buffer (150 mM NaCl, 1% Triton X-100, 0.7% SDS, 500 μM DTT, 10 mM Tris-HCl, 5 mM EDTA) and chromatin was sheared to an average length of 200–900 base-pairs, using a Covaris S220 Ultrasonicator. The chromatin lysate was diluted with SDS-free ChIP lysis buffer. 15μg of antibody was used for YY1 and OCT4 and 3μg of antibody for H3K9me3. The antibody was added to 5μg of sonicated chromatin along with Dynabeads Protein G magnetic beads (Invitrogen) and incubated at 4°C overnight. The beads were washed twice with each of the following buffers: Mixed Micelle Buffer (150 mM NaCl,

1% Triton X-100, 0.2% SDS, 20 mM Tris-HCl, 5 mM EDTA, 65% sucrose), Buffer 200 (200 mM NaCl, 1% Triton X-100, 0.1% sodium deoxycholate, 25 mM HEPES, 10 mM Tris-HCl, 1 mM EDTA), LiCl detergent wash (250 mM LiCl, 0.5% sodium deoxycholate, 0.5% NP-40, 10 mM Tris-HCl, 1 mM EDTA) and a final wash was performed with 0.1X TE. Finally, beads were resuspended in 1X TE containing 1% SDS and incubated at 65°C for 10 min to elute immunocomplexes. The elution was repeated twice and the samples were incubated overnight at 65°C to reverse cross-linking, along with the untreated input (5% of the starting material). The DNA was digested with 0.5 mg/ml Proteinase K for 1 hour at 65°C and then purified using the ChIP DNA Clean & Concentrator kit (Zymo) and quantified with QUBIT. Barcoded libraries were made with NEBNext Ultra II DNA Library Prep Kit for Illumina (New England BioLabs) and sequenced on an Illumina NextSeq 2000 producing 100 bp paired-end reads.

ChIP-seq analysis

After removing the adapters with TrimGalore!, the sequences were aligned to the reference hg19, using Burrows-Wheeler Alignment tool, with the MEM algorithm [63]. Uniquely mapping aligned reads were filtered based on mapping quality (MAPQ > 10) to restrict our analysis to higher quality and likely uniquely mapped reads, and PCR duplicates were removed. Peaks were called for each SVA site using the default parameters, at 5% FDR, with default parameters.

Generation and culturing of SCi-NCCIT stable cell lines

A plasmid with a tetracycline-inducible dCas9-KRAB expression cassette flanked by piggyBac recombination sites was obtained from the Wysocka Lab at Stanford University. This plasmid 'p-dCas9-KRAB' confers constitutive puromycin resistance, allowing for selection of stably transduced clones when co-expressed with the piggyBac transposase plasmid ('p-PB-Transposase', Systems Bioscience). The p-dCas9-KRAB and p-PB-Transposase plasmids were co-transfected into NCCIT cells (ATCC) at 70% confluency using a 6:1 ratio of Fugene HD (Promega) for 48 hours. Two days post-transfection, cells were treated with puromycin selective media at a concentration of 1 µg/mL. Stable clones were isolated and dCas9 expression assessed via Western blot. Next, we obtained a piggyBac transposon plasmid containing the two sgRNAs [20] targeting ~80% of all annotated SVAs in humans termed 'p-sgRNA' (Systems Bioscience). This plasmid constitutively confers dual sgRNA expression and geneticin resistance. The p-sgRNA and p-PB-Transposase plasmids were co-transfected into the NCCIT-dCas9KRAB cells as above. Two days post-transfection cell were treated with geneticin selective media at a concentration of 400 µg/mL. Following antibiotic selection, the NCCIT-dCas9KRAB-SVAsgRNA (SCi-NCCITs) cell line was maintained in ATCC-formulated RPMI media supplemented with 10% tet-free FBS, 1% L-glutamine, 1 µg/mL puromycin, and 400 µg/mL geneticin and incubated at 5% CO₂, 20% O₂ at 37°C. The SCi-NCCITs were seeded to 40% confluency and treated with 2 µg/mL doxycycline (Sigma Aldrich) for 72 hours. For all molecular and genomic CRISPRi experiments, dCas9-KRAB expression was induced with doxycycline for 72 hours.

Western blot

Cells were washed three times in PBS and lysed in radioimmunoprecipitation assay buffer (RIPA buffer) (50 mM Tris-HCl pH7.5, 150 mM NaCl, 1% Igepal, 0.5% sodium deoxycholate, 0.1% SDS 500 µM DTT) with protease inhibitors. Approximately 40 µg of whole cell lysate were loaded in Novex WedgeWell 4–20% Tris-Glycine Gel (Invitrogen) and subject to SDS-PAGE. Proteins were then transferred to a Immun-Blot PVDF membrane

(ThermoFisher) for antibody probing. Membranes were blocked with a 10% BSA in TBST solution for 30 minutes then incubated with primary antibodies in a 5% BSA in TBST, diluted as above. Next, membranes were washed with TBST and incubated with secondary antibodies, diluted as above. Chemiluminescent signal was detected using the Pierce ECL Plus Western Blotting Substrate (ThermoFisher) and an Amersham Imager 680.

RNA extraction and library preparation for RNA sequencing

Cells were lysed in Tri-reagent (Zymo) and total RNA was extracted using Direct-zol RNA Miniprep kit (Zymo) according to the manufacturer's instructions. RNA was quantified using DeNovix DS-11 Spectrophotometer while the RNA integrity was checked on a Bioanalyzer 2100 (Agilent). Only samples with RIN value above 8.0 were used for transcriptome analysis. RNA libraries were prepared using 1 µg of total RNA input using NEB- Next Poly(A) mRNA Magnetic Isolation Module, NEBNext Ultra™ II Directional RNA Library Prep Kit for Illumina and NEBNext Ultra™ II DNA Library Prep Kit for Illumina according to the manufacturer's instructions (New England Biolabs). Paired-end 100 bp reads were generated.

RNA-seq analysis

Reads were aligned to hg19 using STAR v2.567 [64], in 2-pass mode. Bam files were filtered based on alignment quality ($q = 10$) using Samtools [63]. We used the latest annotations obtained from Ensembl to build reference indexes for the STAR alignment. Adapters were removed with TrimGalore! and Kallisto [65] was used to count reads mapping to each gene. We analyzed differential gene expression with DESeq2 [66].

Statistical and genomic analyses

All statistical analyses were performed using BEDTools v2.27.1 [67], DeepTools, and R v4.1.2. Fasta files of the regions of interest were produced using BEDTools v2.27.1 [67]. Shuffled input sequences were used as background. E-values < 0.001 were used as a threshold for significance. Motif analysis of de-repressed SVAs on a repressed SVA background was performed using HOMER [68]. Pathway analysis was performed with Ingenuity-Pathway Analysis Suite (Qiagen Inc., <https://www.qiagenbioinformatics.com/products/ingenuity-pathway-analysis>).

Supporting information

S1 Data. Coordinates of de-repressed SVAs.

(XLSX)

S2 Data. Genes differentially expressed upon CRISPR-mediated repression of the de-repressed SVAs.

(XLSX)

Acknowledgments

The authors are grateful to Dr. Joanna Wysocka's lab for providing the dCas9-KRAB piggyBac plasmid and in particular to Dr. Raquel Fueyo for providing critical support for the SCi-NCCIT CRISPRi line generation. The authors thank the Genomic Facility at The Wistar Institute (Philadelphia, PA) for the Next Generation Illumina Sequencing.

Author Contributions

Conceptualization: Marco Trizzino.

Data curation: Samantha M. Barnada, Andrew Isopi, Daniela Tejada-Martinez, Clément Goubert, Marco Trizzino.

Formal analysis: Samantha M. Barnada, Andrew Isopi, Clément Goubert, Marco Trizzino.

Funding acquisition: Marco Trizzino.

Investigation: Samantha M. Barnada, Andrew Isopi, Sruti Patoori, Luca Pagliaroli, Mason Tracewell, Marco Trizzino.

Project administration: Marco Trizzino.

Supervision: Marco Trizzino.

Validation: Samantha M. Barnada.

Visualization: Samantha M. Barnada.

Writing – original draft: Samantha M. Barnada, Andrew Isopi, Marco Trizzino.

Writing – review & editing: Samantha M. Barnada, Daniela Tejada-Martinez, Clément Goubert, Sruti Patoori, Luca Pagliaroli, Mason Tracewell, Marco Trizzino.

References

1. McClintock B. The Origin and Behavior of Mutable Loci in Maize. *Proc Natl Acad Sci U S A*. 1950; 36: 344–355. <https://doi.org/10.1073/pnas.36.6.344> PMID: 15430309
2. McClintock B. The significance of responses of the genome to challenge. *Science*. 1984; 226: 792–801. <https://doi.org/10.1126/science.15739260> PMID: 15739260
3. Davidson EH, Britten RJ. Regulation of Gene Expression: Possible Role of Repetitive Sequences. *Science*. 1979; 204: 1052–1059. <https://doi.org/10.1126/science.451548> PMID: 451548
4. Jordan IK, Rogozin IB, Glazko GV, Koonin EV. Origin of a substantial fraction of human regulatory sequences from transposable elements. *Trends in Genetics*. 2003; 19: 68–72. [https://doi.org/10.1016/s0168-9525\(02\)00006-9](https://doi.org/10.1016/s0168-9525(02)00006-9) PMID: 12547512
5. Bejerano G, Lowe CB, Ahituv N, King B, Siepel A, Salama SR, et al. A distal enhancer and an ultraconserved exon are derived from a novel retroposon. *Nature*. 2006; 441: 87–90. <https://doi.org/10.1038/nature04696> PMID: 16625209
6. Wang T, Zeng J, Lowe CB, Sellers RG, Salama SR, Yang M, et al. Species-specific endogenous retroviruses shape the transcriptional network of the human tumor suppressor protein p53. *PNAS*. 2007; 104: 18613–18618. <https://doi.org/10.1073/pnas.0703637104> PMID: 18003932
7. Bourque G, Leong B, Vega VB, Chen X, Lee YL, Srinivasan KG, et al. Evolution of the mammalian transcription factor binding repertoire via transposable elements. *Genome Res*. 2008; 18: 1752–1762. <https://doi.org/10.1101/gr.080663.108> PMID: 18682548
8. Kunarso G, Chia N-Y, Jeyakani J, Hwang C, Lu X, Chan Y-S, et al. Transposable elements have rewired the core regulatory network of human embryonic stem cells. *Nat Genet*. 2010; 42: 631–634. <https://doi.org/10.1038/ng.600> PMID: 20526341
9. Lynch VJ, Leclerc RD, May G, Wagner GP. Transposon-mediated rewiring of gene regulatory networks contributed to the evolution of pregnancy in mammals. *Nat Genet*. 2011; 43: 1154–1159. <https://doi.org/10.1038/ng.917> PMID: 21946353
10. Lynch VJ, Nnamani MC, Kapusta A, Brayer K, Plaza SL, Mazur EC, et al. Ancient transposable elements transformed the uterine regulatory landscape and transcriptome during the evolution of mammalian pregnancy. *Cell Rep*. 2015; 10: 551–561. <https://doi.org/10.1016/j.celrep.2014.12.052> PMID: 25640180
11. Schmidt D, Schwalie PC, Wilson MD, Ballester B, Gonçalves Â, Kutter C, et al. Waves of Retrotransposon Expansion Remodel Genome Organization and CTCF Binding in Multiple Mammalian Lineages. *Cell*. 2012; 148: 335–348. <https://doi.org/10.1016/j.cell.2011.11.058> PMID: 22244452
12. Jacques P-É, Jeyakani J, Bourque G. The Majority of Primate-Specific Regulatory Sequences Are Derived from Transposable Elements. *PLOS Genetics*. 2013; 9: e1003504. <https://doi.org/10.1371/journal.pgen.1003504> PMID: 23675311

13. Chuong EB, Rumi MAK, Soares MJ, Baker JC. Endogenous retroviruses function as species-specific enhancer elements in the placenta. *Nat Genet.* 2013; 45: 325–329. <https://doi.org/10.1038/ng.2553> PMID: 23396136
14. Chuong EB, Elde NC, Feschotte C. Regulatory evolution of innate immunity through co-option of endogenous retroviruses. *Science.* 2016; 351: 1083–1087. <https://doi.org/10.1126/science.aad5497> PMID: 26941318
15. Sundaram V, Cheng Y, Ma Z, Li D, Xing X, Edge P, et al. Widespread contribution of transposable elements to the innovation of gene regulatory networks. *Genome Res.* 2014; 24: 1963–1976. <https://doi.org/10.1101/gr.168872.113> PMID: 25319995
16. Trizzino M, Park Y, Holsbach-Beltrame M, Aracena K, Mika K, Caliskan M, et al. Transposable elements are the primary source of novelty in primate gene regulation. *Genome Res.* 2017; 27: 1623–1633. <https://doi.org/10.1101/gr.218149.116> PMID: 28855262
17. Trizzino M, Kapusta A, Brown CD. Transposable elements generate regulatory novelty in a tissue-specific fashion. *BMC Genomics.* 2018; 19: 468. <https://doi.org/10.1186/s12864-018-4850-3> PMID: 29914366
18. Fuentes DR, Swigut T, Wysocka J. Systematic perturbation of retroviral LTRs reveals widespread long-range effects on human gene regulation. Heard E, Weigel D, editors. *eLife.* 2018; 7: e35989. <https://doi.org/10.7554/eLife.35989> PMID: 30070637
19. Ward MC, Zhao S, Luo K, Pavlovic BJ, Karimi MM, Stephens M, et al. Silencing of transposable elements may not be a major driver of regulatory evolution in primate iPSCs. Wittkopp PJ, editor. *eLife.* 2018; 7: e33084. <https://doi.org/10.7554/eLife.33084> PMID: 29648536
20. Pontis J, Planet E, Offner S, Turelli P, Duc J, Coudray A, et al. Hominoid-Specific Transposable Elements and KZFPs Facilitate Human Embryonic Genome Activation and Control Transcription in Naive Human ESCs. *Cell Stem Cell.* 2019; 24: 724–735.e5. <https://doi.org/10.1016/j.stem.2019.03.012> PMID: 31006620
21. Miao B, Fu S, Lyu C, Gontarz P, Wang T, Zhang B. Tissue-specific usage of transposable element-derived promoters in mouse development. *Genome Biology.* 2020; 21: 255. <https://doi.org/10.1186/s13059-020-02164-3> PMID: 32988383
22. Judd J, Sanderson H, Feschotte C. Evolution of mouse circadian enhancers from transposable elements. *Genome Biology.* 2021; 22: 193. <https://doi.org/10.1186/s13059-021-02409-9> PMID: 34187518
23. Mika K, Marinić M, Singh M, Muter J, Brosens JJ, Lynch VJ. Evolutionary transcriptomics implicates new genes and pathways in human pregnancy and adverse pregnancy outcomes. Rokas A, Perry GH, Stevens A, Wildman DE, Mesiano S, editors. *eLife.* 2021; 10: e69584. <https://doi.org/10.7554/eLife.69584> PMID: 34623259
24. Patoori S, Barnada S, Trizzino M. Young transposable elements rewired gene regulatory networks in human and chimpanzee hippocampal intermediate progenitors. 2021 Nov p. 2021.11.24.469877. <https://doi.org/10.1101/2021.11.24.469877>
25. Goubert C, Zevallos NA, Feschotte C. Contribution of unfixed transposable element insertions to human regulatory variation. *Philosophical Transactions of the Royal Society B: Biological Sciences.* 2020; 375: 14. <https://doi.org/10.1098/rstb.2019.0331> PMID: 32075552
26. Ostertag EM, Goodier JL, Zhang Y, Kazazian HH. SVA Elements Are Nonautonomous Retrotransposons that Cause Disease in Humans. *The American Journal of Human Genetics.* 2003; 73: 1444–1451. <https://doi.org/10.1086/380207> PMID: 14628287
27. Cosby RL, Judd J, Zhang R, Zhong A, Garry N, Pritham EJ, et al. Recurrent evolution of vertebrate transcription factors by transposase capture. *Science.* 2021; 371. <https://doi.org/10.1126/science.abc6405> PMID: 33602827
28. Payer LM, Steranka JP, Ardeljan D, Walker J, Fitzgerald KC, Calabresi PA, et al. Alu insertion variants alter mRNA splicing. *Nucleic Acids Research.* 2019; 47: 421–431. <https://doi.org/10.1093/nar/gky1086> PMID: 30418605
29. Lee E, Iskow R, Yang L, Gokcumen O, Haseley P, Luquette LJ, et al. Landscape of Somatic Retrotransposition in Human Cancers. *Science.* 2012; 337: 967–971. <https://doi.org/10.1126/science.1222077> PMID: 22745252
30. Li W, Jin Y, Prazak L, Hammell M, Dubnau J. Transposable Elements in TDP-43-Mediated Neurodegenerative Disorders. *PLOS ONE.* 2012; 7: e44099. <https://doi.org/10.1371/journal.pone.0044099> PMID: 22957047
31. Li W, Prazak L, Chatterjee N, Grüniger S, Krug L, Theodorou D, et al. Activation of transposable elements during aging and neuronal decline in *Drosophila*. *Nat Neurosci.* 2013; 16: 529–531. <https://doi.org/10.1038/nn.3368> PMID: 23563579

32. Pugacheva EM, Teplyakov E, Wu Q, Li J, Chen C, Meng C, et al. The cancer-associated CTCFL/BORIS protein targets multiple classes of genomic repeats, with a distinct binding and functional preference for humanoid-specific SVA transposable elements. *Epigenetics & Chromatin*. 2016; 9: 35. <https://doi.org/10.1186/s13072-016-0084-2> PMID: 27588042
33. Anwar SL, Wulaningsih W, Lehmann U. Transposable Elements in Human Cancer: Causes and Consequences of Dereglulation. *International Journal of Molecular Sciences*. 2017; 18: 974. <https://doi.org/10.3390/ijms18050974> PMID: 28471386
34. Krug L, Chatterjee N, Borges-Monroy R, Hearn S, Liao W-W, Morrill K, et al. Retrotransposon activation contributes to neurodegeneration in a Drosophila TDP-43 model of ALS. *PLOS Genetics*. 2017; 13: e1006635. <https://doi.org/10.1371/journal.pgen.1006635> PMID: 28301478
35. Guo C, Jeong H-H, Hsieh Y-C, Klein H-U, Bennett DA, De Jager PL, et al. Tau Activates Transposable Elements in Alzheimer's Disease. *Cell Reports*. 2018; 23: 2874–2880. <https://doi.org/10.1016/j.celrep.2018.05.004> PMID: 29874575
36. Kong Y, Rose CM, Cass AA, Williams AG, Darwish M, Lianoglou S, et al. Transposable element expression in tumors is associated with immune infiltration and increased antigenicity. *Nat Commun*. 2019; 10: 5228. <https://doi.org/10.1038/s41467-019-13035-2> PMID: 31745090
37. Jang HS, Shah NM, Du AY, Dailey ZZ, Pehrsson EC, Godoy PM, et al. Transposable elements drive widespread expression of oncogenes in human cancers. *Nat Genet*. 2019; 51: 611–617. <https://doi.org/10.1038/s41588-019-0373-3> PMID: 30926969
38. Ivancevic A, Chuong EB. Transposable elements teach T cells new tricks. *PNAS*. 2020; 117: 9145–9147. <https://doi.org/10.1073/pnas.2004493117> PMID: 32312814
39. Ewing AD, Smits N, Sanchez-Luque FJ, Faivre J, Brennan PM, Richardson SR, et al. Nanopore Sequencing Enables Comprehensive Transposable Element Epigenomic Profiling. *Molecular Cell*. 2020; 80: 915–928.e5. <https://doi.org/10.1016/j.molcel.2020.10.024> PMID: 33186547
40. Scott EC, Gardner EJ, Masood A, Chuang NT, Vertino PM, Devine SE. A hot L1 retrotransposon evades somatic repression and initiates human colorectal cancer. *Genome Res*. 2016; 26: 745–755. <https://doi.org/10.1101/gr.201814.115> PMID: 27197217
41. Haring NL, van Bree EJ, Jordaan WS, Roels JRE, Sotomayor GC, Hey TM, et al. ZNF91 deletion in human embryonic stem cells leads to ectopic activation of SVA retrotransposons and up-regulation of KRAB zinc finger gene clusters. *Genome Res*. 2021; 31: 551–563. <https://doi.org/10.1101/gr.265348.120> PMID: 33722937
42. Wang H, Xing J, Grover D, Hedges DJ, Han K, Walker JA, et al. SVA Elements: A Hominid-specific Retroposon Family. *Journal of Molecular Biology*. 2005; 354: 994–1007. <https://doi.org/10.1016/j.jmb.2005.09.085> PMID: 16288912
43. Raiz J, Damert A, Chira S, Held U, Klawitter S, Hamdorf M, et al. The non-autonomous retrotransposon SVA is trans -mobilized by the human LINE-1 protein machinery. *Nucleic Acids Research*. 2012; 40: 1666–1683. <https://doi.org/10.1093/nar/gkr863> PMID: 22053090
44. Tang WWC, Dietmann S, Irie N, Leitch HG, Floros VI, Bradshaw CR, et al. A Unique Gene Regulatory Network Resets the Human Germline Epigenome for Development. *Cell*. 2015; 161: 1453–1467. <https://doi.org/10.1016/j.cell.2015.04.053> PMID: 26046444
45. Molaro A, Hodges E, Fang F, Song Q, McCombie WR, Hannon GJ, et al. Sperm Methylation Profiles Reveal Features of Epigenetic Inheritance and Evolution in Primates. *Cell*. 2011; 146: 1029–1041. <https://doi.org/10.1016/j.cell.2011.08.016> PMID: 21925323
46. Lazaros L, Kitsou C, Kostoulas C, Bellou S, Hatzil E, Ladias P, et al. Retrotransposon expression and incorporation of cloned human and mouse retroelements in human spermatozoa. *Fertility and Sterility*. 2017; 107: 821–830. <https://doi.org/10.1016/j.fertnstert.2016.12.027> PMID: 28139237
47. Georgiou I, Noutsopoulos D, Dimitriadou E, Markopoulos G, Apergi A, Lazaros L, et al. Retrotransposon RNA expression and evidence for retrotransposition events in human oocytes. *Human Molecular Genetics*. 2009; 18: 1221–1228. <https://doi.org/10.1093/hmg/ddp022> PMID: 19147684
48. Gordon S, Akopyan G, Garban H, Bonavida B. Transcription factor YY1: structure, function, and therapeutic implications in cancer biology. *Oncogene*. 2006; 25: 1125–1142. <https://doi.org/10.1038/sj.onc.1209080> PMID: 16314846
49. Pabst T, Mueller BU, Zhang P, Radomska HS, Narravula S, Schnittger S, et al. Dominant-negative mutations of CEBPA, encoding CCAAT/enhancer binding protein- α (C/EBP α), in acute myeloid leukemia. *Nat Genet*. 2001; 27: 263–270. <https://doi.org/10.1038/85820> PMID: 11242107
50. Umek RM, Friedman AD, McKnight SL. CCAAT-Enhancer Binding Protein: A Component of a Differentiation Switch. *Science*. 1991; 251: 288–292. <https://doi.org/10.1126/science.1987644> PMID: 1987644

51. Clapier CR, Cairns BR. The Biology of Chromatin Remodeling Complexes. *Annual Review of Biochemistry*. 2009; 78: 273–304. <https://doi.org/10.1146/annurev.biochem.77.062706.153223> PMID: 19355820
52. Zubenko GS, Hughes HB. Effects of the G(–656)A variant on CREB1 promoter activity in a neuronal cell line: Interactions with gonadal steroids and stress. *Mol Psychiatry*. 2009; 14: 390–397. <https://doi.org/10.1038/mp.2008.23> PMID: 18317463
53. Sirotkin AV, Benčo A, Mlynček M, Harrath AH, Alwaseel S, Kotwica J. The involvement of the phosphorylatable and nonphosphorylatable transcription factor CREB-1 in the control of human ovarian cell functions. *Comptes Rendus Biologies*. 2019; 342: 90–96. <https://doi.org/10.1016/j.crv.2019.03.002> PMID: 31028003
54. Chen M, Zhang L, Cui X, Lin X, Li Y, Wang Y, et al. Wt1 directs the lineage specification of sertoli and granulosa cells by repressing Sf1 expression. *Development*. 2016; dev.144105. <https://doi.org/10.1242/dev.144105> PMID: 27888191
55. Grabowski M, Jungers WL. Evidence of a chimpanzee-sized ancestor of humans but a gibbon-sized ancestor of apes. *Nat Commun*. 2017; 8: 880. <https://doi.org/10.1038/s41467-017-00997-4> PMID: 29026075
56. Meyer TJ, Held U, Nevonen KA, Klavitter S, Pirzer T, Carbone L, et al. The Flow of the Gibbon LAVA Element Is Facilitated by the LINE-1 Retrotransposition Machinery. *Genome Biology and Evolution*. 2016; 8: 3209–3225. <https://doi.org/10.1093/gbe/evw224> PMID: 27635049
57. Okhovat M, Nevonen KA, Davis BA, Michener P, Ward S, Milhaven M, et al. Co-option of the lineage-specific LAVA retrotransposon in the gibbon genome. *PNAS*. 2020; 117: 19328–19338. <https://doi.org/10.1073/pnas.2006038117> PMID: 32690705
58. Fueyo R, Judd J, Feschotte C, Wysocka J. Roles of transposable elements in the regulation of mammalian transcription. *Nat Rev Mol Cell Biol*. 2022 [cited 19 Mar 2022]. <https://doi.org/10.1038/s41580-022-00457-y> PMID: 35228718
59. Sundaram V, Choudhary MNK, Pehrsson E, Xing X, Fiore C, Pandey M, et al. Functional cis-regulatory modules encoded by mouse-specific endogenous retrovirus. *Nat Commun*. 2017; 8: 14550. <https://doi.org/10.1038/ncomms14550> PMID: 28348391
60. Sundaram V, Wysocka J. Transposable elements as a potent source of diverse cis-regulatory sequences in mammalian genomes. *Philosophical Transactions of the Royal Society B: Biological Sciences*. 2020; 375: 20190347. <https://doi.org/10.1098/rstb.2019.0347> PMID: 32075564
61. Takahashi K, Yamanaka S. Induction of Pluripotent Stem Cells from Mouse Embryonic and Adult Fibroblast Cultures by Defined Factors. *Cell*. 2006; 126: 663–676. <https://doi.org/10.1016/j.cell.2006.07.024> PMID: 16904174
62. Weintraub AS, Li CH, Zamudio AV, Sigova AA, Hannett NM, Day DS, et al. YY1 Is a Structural Regulator of Enhancer-Promoter Loops. *Cell*. 2017; 171: 1573–1588.e28. <https://doi.org/10.1016/j.cell.2017.11.008> PMID: 29224777
63. Li H, Handsaker B, Wysoker A, Fennell T, Ruan J, Homer N, et al. The Sequence Alignment/Map format and SAMtools. *Bioinformatics*. 2009; 25: 2078–2079. <https://doi.org/10.1093/bioinformatics/btp352> PMID: 19505943
64. Dobin A, Davis CA, Schlesinger F, Drenkow J, Zaleski C, Jha S, et al. STAR: ultrafast universal RNA-seq aligner. *Bioinformatics*. 2013; 29: 15–21. <https://doi.org/10.1093/bioinformatics/bts635> PMID: 23104886
65. Bray NL, Pimentel H, Melsted P, Pachter L. Near-optimal probabilistic RNA-seq quantification. *Nat Biotechnol*. 2016; 34: 525–527. <https://doi.org/10.1038/nbt.3519> PMID: 27043002
66. Love MI, Huber W, Anders S. Moderated estimation of fold change and dispersion for RNA-seq data with DESeq2. *Genome Biology*. 2014; 15: 550. <https://doi.org/10.1186/s13059-014-0550-8> PMID: 25516281
67. Quinlan AR, Hall IM. BEDTools: a flexible suite of utilities for comparing genomic features. *Bioinformatics*. 2010; 26: 841–842. <https://doi.org/10.1093/bioinformatics/btq033> PMID: 20110278
68. Heinz S, Benner C, Spann N, Bertolino E, Lin YC, Laslo P, et al. Simple Combinations of Lineage-Determining Transcription Factors Prime cis-Regulatory Elements Required for Macrophage and B Cell Identities. *Molecular Cell*. 2010; 38: 576–589. <https://doi.org/10.1016/j.molcel.2010.05.004> PMID: 20513432